Salomón, R. L., De Roo, L., Bodé, S., Boeckx, P., & Steppe, K. (2021). Efflux and assimilation of xylem-transported CO2 in stems and leaves of tree species with different wood anatomy. Plant, Cell and Environment, 44(11), 3494–3508. https://doi.org/10.1111/pce.14062 © 2021 John Wiley & Sons Ltd.

Efflux and assimilation of xylem-transported CO_2 in stems and leaves of tree species with different wood anatomy

Roberto Luis Salomón[1,2], Linus De Roo[1], Samuel Bodé[3], Pascal Boeckx[3], Kathy Steppe[1]

[1] Laboratory of Plant Ecology, Department of Plants and Crops, Faculty of Bioscience Engineering, Ghent University, Coupure links 653, 9000 Ghent, Belgium

[2] Grupo de Investigación Sistemas Naturales e Historia Forestal, Universidad Politécnica de Madrid, Madrid 28040, Spain

[3] Isotope Bioscience Laboratory – ISOFYS, Faculty of Bioscience Engineering, Ghent University, Gent 9000, Belgium

Corresponding author: Roberto L. Salomón; roberto.salomon@upm.es

Running head

Fate of xylem-transported CO_2

Funding

This project received funding from the FWO and the European Union's Horizon 2020 research and innovation programme under the Marie Skłodowska-Curie grant agreement no 665501 granted to R.L.S, as well as from the Special Research Fund (BOF) of Ghent University for Postdoctoral Fellowships. Additionally, funding was provided by the Research Foundation Flanders (FWO) under Research Programme G.0941.15N granted to K.S. and supporting the research of L.D.R.

Acknowledgements

We thank Philip Deman and Geert Favyts for their inestimable help to prepare and maintain the experimental setup. We also thank Katja Van Nieuland for her work on the isotopic analyses and Nancy Pausenberger for isotopic sample preparation.

Data Availability Statement

The data that support the findings of this study are available from the corresponding author upon reasonable request.

Abstract

Determining the fate of CO_2 respired in woody tissues is necessary to understand plant respiratory physiology and to evaluate CO_2 recycling mechanisms. An aqueous ^{13}C-enriched CO_2 solution was infused into the stem of 3-4 m tall trees to estimate efflux and assimilation of xylem-transported CO_2 via cavity ring down laser spectroscopy and isotope ratio mass spectrometry, respectively. Different tree locations (lower stem, upper stem and leafy shoots) and tissues (xylem, bark and leaves) were monitored in species with tracheid, diffuse- and ring- porous wood anatomy (cedar, maple and oak, respectively). Radial xylem CO_2 diffusivity and xylem [CO_2] were lower in cedar relative to maple and oak trees, thereby limiting label diffusion. Part of the labeled $^{13}CO_2$ was assimilated in cedar (8.7 %) and oak (20.6 %) trees, mostly in xylem and bark tissues of the stem, while limited solution uptake in maple trees hindered detection of label assimilation. Little label reached foliar tissues, suggesting substantial label loss along the stem-branch transition following reductions in the radial diffusive pathway. Differences in respiration rates and radial xylem CO_2 diffusivity (lower in conifer relative to angiosperm species) might reconcile discrepancies in efflux and assimilation of xylem-transported CO_2 so far observed between taxonomic clades.

Keywords

Carbon allocation, CO_2 diffusion, CO_2 recycling, ^{13}C-CO_2 labelling, plant respiration, stem CO_2 efflux, woody tissue photosynthesis, xylem CO_2 transport

Introduction

Understanding the fate of CO_2 respired in woody tissues is necessary to predict total plant respiration (Teskey, Saveyn, Steppe & McGuire 2008; Trumbore, Angert, Kunert, Muhr & Chambers 2013; Salomón, De Roo, Oleksyn, De Pauw & Steppe 2020), which largely determines ecosystem carbon (C) use efficiency and is a key component of ecosystem and global C balances (Valentini *et al.* 2000; Yang, He, Aubrey, Zhuang & Teskey 2016; Huntingford *et al.* 2017). However, this is a challenging task as respiration in plants is not directional. Measurements of CO_2 efflux should not be used as a surrogate of the respiratory activity of tissues underneath; especially in non-apical woody organs, where respired CO_2 is not necessarily emitted to the atmosphere following diffusion gradients. In roots, stems and branches, respired CO_2 can dissolve in the sap solution and be transported through the xylem (Teskey *et al.* 2008), passively diffuse in the axial direction (De Roo, Bloemen, Dupon, Salomón & Steppe 2019), or be re-assimilated via photosynthetic (Ávila, Herrera & Tezara 2014) and anaplerotic (Hilman *et al.* 2019) reactions. Uncertain fate of respired CO_2 in woody tissues is therefore responsible for substantial bias in root (Aubrey & Teskey 2009; Bloemen, Teskey, McGuire, Aubrey & Steppe 2016), stem (Hölttä & Kolari 2009; Teskey, McGuire, Bloemen, Aubrey & Steppe 2017) as well as leaf (Stutz, Anderson, Zulick & Hanson 2017) respiration estimates.

A common approach to track CO_2 movement within plants is to irrigate or infuse different organs (roots, stems, detached branches or petioles) with an isotopically labelled HCO_3^- solution and subsequently detect the label emitted to the atmosphere or assimilated by organs and tissues. A majority of studies, mostly performed in angiosperm species, have reported a substantial effect of xylem-transported CO_2 on the emission of CO_2 downstream from the point of label infusion. Xylem-transported CO_2 accounted for 12-44% of CO_2 efflux in *P. tremula* branches and stems (Salomón, De Roo, Bodé, Boeckx & Steppe 2019; Mincke, Courtyn, Vanhove, Vandenberghe & Steppe 2020); whereas xylem-transported CO_2 was up to 50% of the amount of leaf respiration in *Brassica napus* and *Populus deltoides* (Stutz *et al.* 2017). In conifer species, however, inconsistent patterns have been reported. Large conifer trees of three species irrigated with a ^{13}C-enriched HCO_3^- solution showed negligible isotopic enrichment in the xylem CO_2 gas pool and

in stem CO_2 efflux (Ubierna *et al.* 2009). A $^{13}CO_2$ labelling pulse into the xylem of a *Thuja occidentalis* tree did result in ^{13}C enrichment of the xylem CO_2 gas pool (Powers & Marshall 2011). Recently, $^{13}CO_2$ infused at the stem base of *Pinus sylvestris* trees rapidly diffused to the atmosphere, largely limiting the amount of label reaching the canopy (Tarvainen *et al.* 2020). Radial xylem CO_2 diffusivity is a key trait determining the fate of xylem-transported CO_2, and differences between species with tracheid, ring- or diffuse-porous wood anatomy (Sorz & Hietz 2006) may partially explain such contrasting observations between conifer and angiosperm species. Nevertheless, literature on radial xylem CO_2 diffusivity is scarce, and commonly derived from Fick´s law of diffusion applying measurements of stem CO_2 efflux and xylem [CO_2] (Steppe, Saveyn, McGuire, Lemeur & Teskey 2007; Teskey *et al.* 2008; Salomón *et al.* 2016). This approach, however, may systematically overestimate diffusivity, as CO_2 respired by tissues located outside the cambium layer rapidly diffuses to the atmosphere facing minimal resistance. In this line, C tracking could provide more accurate estimates of the diffusion flux from the xylem tissues, hereby refining diffusivity estimates.

Understanding the fate of respired CO_2 in plants is not only relevant to advance knowledge on the regulation and quantification of plant respiration. Respired CO_2 within woody tissues might constitute a qualitatively important C source for plant functioning under drought stress, when leaf assimilation of exogenous CO_2 is limited due to stomatal closure (Vandegehuchte, Bloemen, Vergeynst & Steppe 2015; Stutz & Hanson 2019; De Roo, Salomón & Steppe 2020b). Following isotopic and non-isotopic approaches, woody tissue photosynthesis has been observed to widely occur across plant functional types and lineages (Ávila *et al.* 2014). Labelled $^{13}CO_2$ dissolved in the xylem sap solution was recovered in xylem and bark tissues located downstream of the point of infusion in both angiosperm (McGuire, Marshall & Teskey 2009; Bloemen *et al.* 2013a; Bloemen, McGuire, Aubrey, Teskey & Steppe 2013b; Mincke *et al.* 2020) and conifer (Ford, Wurzburger, Hendrick & Teskey 2007; Powers & Marshall 2011; Tarvainen *et al.* 2020) species. Larger isotopic enrichment has been commonly observed in the bark (integrating cambium, phloem and periderm tissues) relative to the xylem, as chloroplast-containing cells are mostly located in peripheral layers where

light transmission is sufficient to trigger photosynthetic light reactions. Discrepancies regarding the potential of CO_2 recycling at the leaf level arise again between taxonomic clades. Assimilation of xylem-transported CO_2 by leaves has been observed in angiosperm *Populus* spp. (Stringer & Kimmerer 1993; Bloemen *et al.* 2013a b, 2015; Hubeau *et al.* 2019; Stutz & Hanson 2019) and *Platanus occidentalis* (McGuire *et al.* 2009); whereas it seems to be limited or even absent in conifer *Pinus* spp. (Ford *et al.* 2007; Tarvainen *et al.* 2020) and *Thuja occidentalis* (Powers & Marshall 2011).

The goal of this study is to track the fate of xylem-transported CO_2 in species with different wood anatomy including a conifer species with tracheid anatomy and angiosperm species with diffuse- and ring-porous anatomy. For that, a labelled HCO_3^- solution enriched in ^{13}C was infused at the stem base of six trees per species as a surrogate of root respired CO_2 dissolved in sap (Bloemen *et al.* 2013a). Subsequently, real-time measurements of CO_2 concentration ($[CO_2]$) and ^{13}C abundance ($a^{13}C$) in CO_2 efflux throughout the plant, from woody stems to leafy shoots, were performed via Cavity Ring Down Laser Spectroscopy (CRDS). Tissue ^{13}C enrichment after the labelling period was measured via isotope-ratio mass spectrometry across tree locations and tissues (xylem, bark and leaves), and up-scaled to the whole tree accounting for biomass allocation. An identical protocol of label infusion and detection will therefore facilitate straightforward inter-specific comparison of CO_2 movement within the plant to assess differences in efflux and assimilation of xylem-transported CO_2. We hypothesize that radial xylem CO_2 diffusivity, estimated by means of an isotopic mass balance, largely determines the fate of respired CO_2 within the plant: (1) efflux of xylem-transported CO_2 will be directly related to radial xylem CO_2 diffusivity, and (2) assimilation of xylem-transported CO_2 will depend on the concentration of CO_2 in the xylem, being therefore inversely related to its radial diffusivity.

Materials and methods

Experimental setup and labelling procedure

Trees of three species with different wood anatomy were instrumented to monitor efflux and assimilation of xylem-transported CO_2. White cedar (*Thuja occidentalis* L. 'Smaragd'), Norway maple (*Acer platanoides*

L. 'Crimson King') and pedunculate oak (*Quercus robur* L.) were selected as species with tracheid-, diffuse-porous and ring-porous wood anatomy, respectively. Six trees per species were grown outdoors and moved by sets into the glasshouse facilities of Ghent University along the growing season of 2017 during the 6-10 days period of CRDS, sap flow and xylem [CO_2] measurements (see below). Trees were divided into six measurement sets consisting of three trees of the same species each to be sequentially monitored during spring and late summer, after leaf emergence and before visual symptoms of leaf senescence were observed, respectively, in the case of deciduous species. Table 1 displays the timing (days of the year) in which measurement sets were monitored. Trees were watered on a daily basis with an automated irrigation system to avoid drought stress, both outdoors and inside the glasshouse. Before measurements started, average tree height and diameter at the stem base was c. 3 m and 5-6 cm for cedar trees and c. 4 m and 3.5-4.5 cm for maple and oak trees, respectively.

Labelling was performed following the protocol initially described by Bloemen *et al.* (2013a) and later refined by Salomón *et al.* (2019). Briefly, we prepared a 5.88 mM $NaH^{13}CO_3$ ($a^{13}C$ = 98%, Sigma Aldrich, Overijse, Belgium) solution, corresponding to the average concentration of dissolved inorganic carbon (DIC) in the sap solution reported across species (Teskey *et al.* 2008), in deionized water with 40 mM KCl. The resulting basic solution (pH ≈ 8.3) minimizes label gasification and loss during labelling, and once the solution is infused into the xylem sap (slightly acidic), equilibrium reactions shift toward the formation of aqueous CO_2, and subsequently gaseous CO_2 according to Henry's law (McGuire & Teskey 2002; Powers & Marshall 2011). Label solution was prepared the day before infusion and stored at 4 ºC in high-density polyethylene bottles. Label solution was infused through two small holes located at opposite sides of the stem drilled 10-15 cm above soil level (see Figure 1a for a photograph of the setup). Two bottles per tree (one per hole) were suspended c. 1.5 m above soil level to induce a head pressure for solution uptake. Stem holes were 20 mm long and metallic threaded fittings connected to the bottles via tubing were drilled 10 mm into the stems to facilitate sapwood contact with the solution and to ensure tight contact along the stem-fitting interface, hereby avoiding leaks. Measurements of sapwood depth were performed *a priori* in

ancillary trees to ensure that holes did not reach the sapwood-heartwood boundary. There was no heartwood in maple and oak trees. Labelling lasted 4-5 days, and solution uptake was measured on a daily basis based on mass of the reservoir. Bottles were refilled before they were empty to allow continuous solution uptake.

CO_2 gas exchange in stems and shoots

Four locations were selected to sample CO_2 exchange (Figure 1a): one stem segment located c. 45 cm above soil level, a second stem segment located just below the first branch (hereafter ´lower and upper stem´, respectively) and two leafy shoots from the 25% lowermost and uppermost part of the canopy (hereafter ´lower and upper shoot´, respectively). Stem CO_2 efflux was sampled following Salomón *et al.* (2019). Briefly, custom-made cuvettes enclosing 15 cm-length stem segments were made of flexible polycarbonate film and sealed with adhesive foam gaskets and non-caustic silicone. Cuvettes were covered with aluminium foil to avoid local woody tissue photosynthesis. Shoot CO_2 exchange (including photosynthetic and respiratory fluxes) was sampled following De Roo *et al.* (2020a), using custom-made, air-tight and transparent plastic bags sealed with stripes mounted over malleable polysiloxane material (Terostat-IX, Henkel AG & Company, Germany) to avoid mechanical girdling. A reference cuvette enclosing a PVC pipe was integrated within the setup to account for variation in ambient [CO_2] and $a^{13}C$ inside the glasshouse. Stem cuvettes and shoot bags (´chambers´ hereafter) were flushed continuously with ambient air, mixed in 50-L containers for ambient [CO_2] stabilization, at an average rate of 0.997 L min^{-1}. Air flow through chambers was measured with flow meters (model 5860S; Brooks Instruments, Ede, The Netherlands) placed before the chamber inlet. For measurement, a portion of air flux exiting the monitored chamber was deviated to the analyser using a custom-made multiplexer switching between chambers every five minutes. A multiplexer with 13 channels (3 trees × 4 locations + reference cuvette) was initially envisaged; however, due to malfunction of two channels, upper shoots were uniquely monitored in one tree per measurement set, and every chamber was monitored every 55 minutes (11 channels × 5 minutes). Readings from the three last minutes were considered to allow CO_2 to stabilize. A Cavity Ring Down Laser Spectroscopy isotopic-CO_2 gas analyser (Model G2131-I, Picarro Inc., Santa Clara, CA, USA) was used to measure [CO_2] and

$a^{13}C$ of sampled CO_2. See Dickinson *et al.* (2017) for a detailed description on the gas analyses procedure. Continuous series of $[CO_2]$ and $a^{13}C$ were obtained by data interpolation between consecutive measurement cycles.

Stem CO_2 efflux and radial xylem CO_2 diffusivity

Stem CO_2 efflux to the atmosphere (E_A, µmol m^{-2} s^{-1}) was estimated following the standard protocol (Long & Hällgren 1993):

$$E_A = \frac{\Delta CO_2 \times P}{R \times T} \frac{f_c}{S} \quad \text{Eqn. 1}$$

where ΔCO_2 is the difference in $[CO_2]$ (ppm) exiting and entering the stem cuvette, with incoming CO_2 being measured in the reference cuvette, P (atm) is the ambient pressure, R (atm mL mol^{-1} K^{-1}) is the universal gas constant, T (K) is air temperature, f_c (mL s^{-1}) is the registered flow through the cuvette, and S (m^2) is the axial surface of the stem segment.

To estimate radial xylem CO_2 diffusivity, distinction between locally-respired and xylem-transported CO_2 in E_A is necessary, so that locally-respired CO_2 by outer tissues (immediately diffusing to the atmosphere) can be excluded from calculation (see discussion). For this, only data from the lower cuvette was considered as the two points of label infusion were located immediately below the lower cuvette (< 5 cm; see Figure 1a), and label loss is expected to be minimal due to their spatial proximity. Contribution of xylem-transported CO_2 (T_{CO2}) to E_A was calculated with an isotopic mass balance according to the mixing of the label solution and the sap solution:

$$T_{CO2}/E_A = (a^{13}C_{EA} - a^{13}C_{LR}) / (a^{13}C_{XT} - a^{13}C_{LR}) \quad \text{Eqn. 2}$$

where $a^{13}C_{EA}$, $a^{13}C_{LR}$ and $a^{13}C_{XT}$ are the ^{13}C abundances in E_A, in locally-respired CO_2 and in xylem-transported CO_2, respectively. $a^{13}C_{EA}$ is estimated as follows:

$$a^{13}C_{EA} = ([CO_2]_{out} \times a^{13}C_{CO2,out} - [CO_2]_{in} \times a^{13}C_{CO2,in}) / ([CO_2]_{out} - [CO_2]_{in}) \quad \text{Eqn. 3}$$

where $[CO_2]_{in}$ and $[CO_2]_{out}$ are the CO_2 incoming and exiting the chamber, and $a^{13}C_{CO2,in}$ and $a^{13}C_{CO2,out}$ the corresponding abundances (all measured via CRDS). $a^{13}C_{LR}$ was estimated likewise from CRDS measurements before label infusion and was assumed constant, as variation in $a^{13}C$ at natural abundance is negligible relative to labelling exercises. $a^{13}C_{XT}$ was estimated by taking into account the fraction of the DIC in xylem derived from the label solution (F_{lab}) and (non-labelled) sap ($F_{sap} = 1 - F_{lab}$), respectively, and their corresponding ^{13}C abundances ($a^{13}C_{lab}$ and $a^{13}C_{sap}$):

$$a^{13}C_{XT} = F_{lab} \times a^{13}C_{lab} + (1 - F_{lab}) \times a^{13}C_{sap} \quad \text{Eqn. 4}$$

$$F_{lab} = \frac{W_{lab} \times [DIC]_{lab}}{W_{lab} \times [DIC]_{lab} + W_{sap} \times [DIC]_{sap}} \quad \text{Eqn. 5}$$

where W_{lab} and W_{sap} (L day^{-1}) are label solution uptake and (non-labelled) sap flow (estimated as the difference between total sap flow measured above the infusion point (W_{tot}) minus W_{lab}), and $[DIC]_{lab}$ and $[DIC]_{sap}$ (mol L^{-1}) is the concentration of DIC in the label solution and in (non-labelled) sap. Ancillary data of $[DIC]_{sap}$ and W_{tot} were therefore necessary to estimate $a^{13}C_{XT}$. Xylem $[CO_2]$ in the gas phase (%) was measured with solid-state non-dispersive infrared (NDIR) sensors (model GMM221, Vaisala, Finland) in ancillary (non-labelled) trees used for intrusive measurements and in two stem locations separated vertically 35-40 cm. Together with measurements of stem temperature and pH, xylem $[CO_2]$ (in the gas phase) was converted into $[DIC]_{sap}$ (in the liquid phase) according to Henry´s law (McGuire & Teskey 2002). Total sap flow in labelled trees (W_{tot}) was measured via the heat ratio method (SFM1, ICT international, Armidale NSW, Australia) in cedar, and via the stem heat balance method (SGB35-WS, Dynagage, Dynamax, Houston, TX, USA) in maple and oak. See Salomón *et al.* (2020) for measurement details of ancillary variables.

Finally, radial xylem CO_2 diffusivity (m^2 s^{-1}) was estimated according to Fick´s law of diffusion (Teskey *et al.* 2008):

$$\text{Diffusivity} = \frac{T_{CO2} \times L}{[CO_2]_{xylem} - [CO_2]_{atm}} \quad \text{Eqn. 6}$$

where T_{CO2} (µmol m^{-2} s^{-1}) is the amount of xylem-transported CO_2 diffusing to the atmosphere estimated as $E_A \cdot T_{CO2}/E_A$, $[CO_2]_{xylem}$ and $[CO_2]_{atm}$ (µmol m^{-3}) are the CO_2 concentration in the gas phase in the xylem and in the glasshouse atmosphere, respectively, and L (m) is the length of the diffusive pathway estimated as half of the sapwood thickness. Note that $[CO_2]_{xylem}$ was back-transformed from $[DIC]_{sap}$ applying Henry´s law to account for the mixing of DIC infused with the label solution and naturally occurring in the sap solution.

Tissue ^{13}C enrichment

Samples for isotopic analyses were collected one day after solution uptake cessation, time enough for infused label to be transported to the top of the canopy according to measured sap flow rates. Samples were taken from three locations: in the stem at mid-way between cuvettes, and in the lower and upper shoots. An increment stem borer and pruning shears were used to sample stems and shoots, respectively. At each location, xylem sapwood and bark tissues were separated manually. Xylem heartwood, only observed in cedar trees, was not sampled due to its negligible potential for photosynthetic assimilation. Leaves from lower and upper shoots were also sampled. Samples were immediately frozen in liquid nitrogen to stop metabolic activity and stored at -80 °C until analysis. Prior to analysis, samples were oven dried at 70 °C for 48 h, milled, and acid-washed to remove ^{13}C-bicarbonate. For this, c.a. 100 mg of sample was placed in a 2 ml plastic container. After addition of 150 µL of ultrapure water the samples were placed in a vacuum desiccator (5 L) containing a beaker with 50 mL of 12 M HCl. The desiccator was vacuum-sealed and samples were exposed to HCl vapour for 24 hours. After removal of the beaker containing HCl, the desiccator was evacuated and filled with air repeatedly for 1 h to remove most HCl vapour. The samples were dried at 60°C for 24 h in an oven containing a beaker of NaOH to trap HCl fumes. After cooling in a desiccator, samples were manually disrupted to a fine powder.

About 3 mg samples were weighed in tin capsules to be analysed with an elemental analyser (ANCA-GSL, PDZ Europa, UδK) interfaced with an isotope ratio mass spectrometry detector (20-22 IRMS, SerCon, Cheshire, UK) to determine sample ^{13}C abundance, expressed here as the difference in isotopic ratio (^{13}R =

239 $^{13}C/^{12}C$) relative to the ^{13}R of the international reference standard VPDB ($\delta^{13}C_{vsVPDB}$). To assess label
240 incorporation into the tissue, the change in $a^{13}C$ compared to the baseline was estimated. However, as
241 observed isotopic enrichments of the plant tissues were very low, the enrichment was also expressed using
242 a relative scale $\delta^{13}C_{vs\ baseline}$:

243 $$\delta^{13}C_{vs\ baseline} = (^{13}R_{sample} / {}^{13}R_{baseline}) - 1 \quad \text{Eqn. 7}$$

244 Baseline samples were taken from a non-labelled tree used for ancillary measurements and located next to
245 labelled trees to account for potential ^{13}C enrichment derived from assimilation of ^{13}C in the glasshouse
246 atmosphere after emission from labelled trees (McGuire *et al.* 2009).

247 To estimate the amount of label assimilated at the whole-tree level, label assimilation throughout tree
248 locations and tissues was estimated as follows:

249 $$Label\ assimilated = DM \times [C] \times \left(\frac{a^{13}C_{sample} - a^{13}C_{baseline}}{a^{13}C_{label} - a^{13}C_{baseline}}\right) \quad \text{Eqn. 8}$$

250 where DM (g) and [C] (unitless) are dry mass and the carbon content of the corresponding tissue and
251 location, respectively, and $a^{13}C_{sample}$, $a^{13}C_{baseline}$ and $a^{13}C_{label}$ are ^{13}C abundances in tissue sample, baseline
252 and in the label (0.98), respectively.

253 Trees were harvested to quantify DM throughout locations (stem, lower shoot and upper shoot) and tissues
254 (heartwood, xylem, bark and leaves) according to the tissue sampling design. Stem biomass of xylem and
255 bark was estimated as the product of fresh volume and dry density. Stem fresh volume of xylem and bark
256 was determined by measuring stem diameter, sapwood depth and bark thickness in two perpendicular
257 directions along the stem at one meter intervals. Dry density of xylem and bark was determined as the ratio
258 between dry mass and fresh volume in stem subsamples. Tree canopy was divided into two halves. Leaf
259 DM in the lower and upper canopy was estimated from measurements of total fresh weight after leaf
260 detachment and the average leaf water content measured in a subsample of six leaves per tree. Dry weight
261 of sampled leaves was measured after drying at 70 °C for 48 h. Similarly, leafless shoot DM in the lower
262 and upper canopy was estimated from measurements of total fresh weight and the average shoot water

content measured in a subsample of two shoots per tree. To partition shoot DM between xylem and bark, a specific linear relationship was established between branch diameter at the junction with the stem and the portion of bark volume relative to total branch volume (%). For this, coaxial conical shapes of shoot xylem and bark were assumed accounting for measured bark thickness and total branch diameter ($n = 12$; R^2 = 0.68, 0.81 and 0.62 for cedar, maple and oak, respectively). Specific allometric relationships were applied to each branch throughout the canopy.

Data analyses

Statistical analyses were performed using R software (R Core Team 2019). To evaluate differences in stem label efflux among species and locations (lower and upper stem) accounting for heterogeneous label solution uptake, the relationship between stem label efflux and label infused was compared with linear mixed models. Species, stem location and their interaction were considered as fixed effects, whereas individual tree was considered a random slope factor. Data from spring and late summer seasons was pooled, as potential differences related to variability in stem growth, associated respiratory costs and natural $a^{13}C$ in E_A are negligible in labelling exercises. *Post-hoc* Tukey´s test was applied for pairwise slope comparison. Significance of tissue enrichment ($\delta^{13}C_{vs\ baseline}$) was individually determined per sample according to the limit of detection (LoD) estimated from the standard deviation of $\delta^{13}C$ in baseline samples ($LoD = 2 \times 1.65 \times SD_{baseline}$). Additionally, comparison of tissue enrichment among species, locations and tissues were performed as indicated above to account for heterogeneous label solution uptake. For this, the relationship between label infused and $\delta^{13}C_{vs\ baseline}$ was adjusted with linear mixed models considering individual tree as a random slope factor.

Finally, and to close the budget of label recovery, the portion of label efflux and label assimilated relative to the total amount of label infused was estimated. Values of label infused, label efflux and label assimilated were averaged per species ($n = 6$) to avoid biased ratios towards those individuals which took up minute label solution. Label efflux (μmol m^{-2} s^{-1}) from the stem was calculated following an isotopic mass balance:

$$Label\ efflux = E_A \times \left(\frac{a^{13}C_{EA} - a^{13}C_{LR}}{a^{13}C_{label} - a^{13}C_{LR}}\right)$$ Eqn. 9

To upscale label efflux from the stem, label efflux rates in the lower and upper cuvettes (on a surface basis) were multiplied by the axial surface of the lower and upper halves of the stem, respectively. Label assimilated at the whole tree level was estimated as the sum of label assimilated throughout tree locations and tissues (Eqn. 8) when significant positive enrichment was observed ($\delta^{13}C_{vs\ baseline}$ > LoD). Mean ± SE values are reported.

Results

Label solution uptake, stem and shoot ε, and radial xylem CO_2 diffusivity

Label solution uptake substantially varied among and within species (Figure 1b). Whereas label solution uptake in cedar trees was 0.525 ± 0.123 L tree^{-1} day^{-1}, it was limited in maple trees with only 0.071 ± 0.010 L tree^{-1} day^{-1}. Mean label solution uptake in oak trees was 0.403 ± 0.178 L tree^{-1} day^{-1}, with substantial differences between spring and late summer measurement sets. Moreover, higher sap flow during spring relative to late summer (data not shown) led to seasonal differences in the contribution of solution uptake to sap flow (Figure S1). Abundance of ^{13}C in air exiting the chambers ($a^{13}C_{CO2,out}$) was largely affected by label solution uptake across measurement sets (Figure 2; note different scales in y–axes) and by tree location. In stem segments and on a sub-daily temporal scale, lower and upper stem showed roughly synchronized $a^{13}C_{CO2,out}$ dynamics in cedar trees during late summer and in oak trees, with higher $a^{13}C_{CO2,out}$ during day-time. Opposite sub-daily $a^{13}C_{CO2,out}$ dynamics were observed between lower and upper stem sections in cedar trees during spring and in maple trees, with the lower stem registering greater $a^{13}C_{CO2,out}$ during night-time. In leafy shoots, sub-daily variation in $a^{13}C_{CO2,out}$ after labelling was similar to that observed before labelling.

The relationship between daily label solution uptake and daily stem label efflux is shown in Figure 3. In the lower stem, the slope of this relationship was lower in cedar trees compared to oak trees ($P < 0.01$). This slope did not change significantly with stem height for cedar ($P > 0.05$), while it did for oak ($P < 0.001$). As a result, no significant differences in the slope were observed between cedar and oak trees in the upper stem

311 ($P > 0.05$). The slope in maple trees did not show significant differences with cedar or oak at any stem
312 location ($P > 0.05$). Negligible variation in $a^{13}C_{CO2,out}$ in leafy shoots after labelling precluded estimation of
313 leaf label efflux. Radial xylem CO_2 diffusivity differed among species ($P < 0.001$, Figure 4); it was lowest
314 for cedar, intermediate for oak and highest for maple (6.86×10^{-10}, 2.22×10^{-9} and 3.63×10^{-9} m^2 s^{-1},
315 respectively). No significant effect of the season (or the season × species interaction) could be seen on
316 diffusivity estimates ($P > 0.05$). Xylem [CO_2] measured in ancillary trees to estimate diffusivity is shown in
317 Figure 5. Mean xylem [CO_2] across seasons and stem locations was 3.5, 8.8 and 12.2 % for cedar, maple
318 and oak, respectively.

319 *Tissue enrichment and overall fate of xylem-transported CO_2*

320 Standard deviation of $\delta^{13}C$ in baseline samples averaged across species, tissues and locations was 0.57 ‰
321 , hence resulting in a limit of detection of 1.88 ‰. Of the 144 potentially enriched samples (3 species × 6
322 trees × 8 samples), positive significant enrichment was detected in 22 samples ($\delta^{13}C_{vs\ baseline} > LoD$, Figure
323 6), most of them in oak and cedar trees in both xylem and bark tissues located in the stem and the lower
324 canopy. Models were adjusted to further evaluate the influence of label solution uptake on tissue enrichment.
325 This relationship was only significant for oak trees, for which the largest gradient in infused label was
326 achieved. Positive relations were observed in bark tissues of stem and shoots, as well as in the xylem of
327 shoots ($P < 0.05$), but not in the xylem of the stem nor in leaves ($P > 0.05$). In cedar and maple trees, this
328 relationship was not significant for any location or tissue ($P > 0.05$).

329 Dry biomass of cedar, maple and oak trees was 4.74 ± 0.25, 2.63 ± 0.06 and 2.76 ± 0.13 kg, respectively
330 (Figure 7a). Although average label solution uptake in cedar and oak trees was comparable (Figure 1b),
331 label assimilated at the whole tree level by oak (31.27 ± 7.28 mg C) more than doubled that of cedar (14.00
332 ± 8.39 mg C; Figure 7b). In maple trees, label assimilation at the whole tree level was undetectable ($\delta^{13}C_{vs}$
333 $_{baseline} < LoD$), likely due to minute solution uptake, and consequently an assimilation potential below 21
334 ppm of biomass C pools (corresponding to the 1.88 ‰ LoD) throughout tree tissues and locations. Most

label assimilation in cedar and oak trees occurred in the stem (> 91 %). In cedar trees, stem xylem and bark tissues accounted for 61 and 30 % of label assimilation, respectively, with the remaining label being detected in xylem and bark tissues of the lower canopy. In oak trees, stem xylem and bark tissues accounted for 47 and 48 % of label assimilation, respectively, with the remaining label being detected in xylem and bark tissues of the lower canopy. Note that for oak trees, however, assimilation in stem xylem tissues might be underestimated as we failed to measure $\delta^{13}C$ in samples of the two oaks with greatest label solution uptake (Figure 6).

The fraction of the infused label allocated into different C sinks was estimated by means of integrating data of stem label efflux (Figure 3) and label assimilation (Figure 7b). In cedar trees, 18.5 % and 16.7 % of the label effluxed to the atmosphere along the lower and upper stem, respectively, whereas 8.7 % was assimilated (Figure 8). Most of the label (56.0 %) remained therefore undetected, likely lost to the atmosphere along woody organs within the canopy (branches). In maple trees, most of the label was lost along the stem (74.1 and 23.0 % in the lower and upper stem, respectively), whereas 2.8 % was undetected. In oak trees, label efflux along the lower and upper stem, and label assimilation accounted for 49.8, 11.2 and 20.6 % of the label infused, respectively, with 18.4 % of the label remaining undetected.

Discussion

Efflux of xylem-transported CO_2

Label solution uptake largely differed among species and seasons, which might be determined by the tree´s ability to refill embolized conduits under positive pressure after hole drilling (De Baerdemaeker *et al.* 2019). It is hypothesized that refilling potential is directly related to xylem conducting efficiency and thus vulnerability to embolism (Ogasa, Miki, Murakami & Yoshikawa 2013; Klein *et al.* 2018). Refilling potential might therefore be determined by conduit traits, which differ among species and can change along the season, particularly in ring-porous species, as suggested here by remarkable seasonal differences in label solution uptake observed in oak trees. This is, however, a controversial topic in the field of plant hydraulics out of the scope of this study. We also suspect that maple exudates, observed after shoot excision for water

potential measurements (Salomón *et al.* 2020), might have contributed to effectively seal open vessels hence limiting solution uptake. Regardless of the cause of heterogeneous label solution uptake, $a^{13}C$ in air exiting stem chambers ($a^{13}C_{CO2,out}$) clearly increased with label solution uptake, whereas variability in $a^{13}C_{CO2,out}$ for the lower shoot was negligible (Figure 2), suggesting that little label, if any, reached foliar tissues, as similarly observed in detached branches of *P. occidentalis* (McGuire *et al.* 2009) and in mature *P. sylvestris* trees (Tarvainen *et al.* 2020). Sub-daily $a^{13}C_{CO2,out}$ dynamics differed among species and (in some sets) with stem height. In upper stem locations, $a^{13}C_{CO2,out}$ consistently increased during day-time, when label solution uptake was largest, hereby facilitating subsequent radial diffusion of xylem-transported $^{13}CO_2$. Depletion of stem water pools during day-time (Steppe, Sterck & Deslauriers 2015) may also facilitate stem label efflux according to sub-daily CO_2 diffusivity dynamics (Salomón *et al.* 2020). Unexpectedly, lower stem locations of cedar trees during spring and maple trees showed an opposite pattern; i.e., $a^{13}C_{CO2,out}$ was lower during day-time. In these cases, the contribution of label solution to total sap flow was limited (below 15%, Figure S1), and dilution of the label solution in soil water coming from the roots during high-transpiration hours together with a low buffering capacity of xylem sap might have facilitated rapid label transport upwards as soluble bicarbonate, thereby partially explaining relatively low $a^{13}C_{CO2,out}$ near the infusion point. We suggest that equilibrium reactions may underpin any spatial and temporal interaction observed in sub-daily dynamics of label diffusion.

On a daily basis, label efflux was directly related to label solution uptake in all monitored species and stem locations (Figure 3). To estimate radial xylem CO_2 diffusivity of stem tissues, Fick´s law of diffusion (Eqn. 6) has been previously applied using E_A as a proxy of the diffusion flux (Steppe, Saveyn, McGuire, Lemeur & Teskey 2007; Teskey *et al.* 2008; Salomón *et al.* 2016). However, E_A overestimates the diffusion flux from the xylem and hence diffusivity estimates. Locally-respired CO_2 in tissues located outside the cambium, which can account for a large fraction of E_A (Maier & Clinton 2006; Salomón, De Schepper, Valbuena-Carabaña, Gil & Steppe 2018), faces minimal diffusive resistance by bark air-filled spaces and minimal diffusive distance, and it is therefore rapidly emitted to the atmosphere. Applying an isotopic mass

385 balance, the contribution of locally-respired CO_2 to E_A can be discarded, thereby improving radial xylem
386 CO_2 diffusivity estimates. Further refinement would be achieved by accounting for locally-respired CO_2 by
387 xylem parenchyma (to be added to xylem-transported CO_2) to more accurately estimate the diffusion flux
388 from xylem tissues. Nevertheless, this potential bias might be relatively small here, as suggested by
389 consistent diffusivity estimates obtained during spring and late summer, because most of the locally respired
390 CO_2 in our young growing trees likely comes from the outer tissues (Fan, McGuire & Teskey 2017),
391 metabolically more active. Radial xylem CO_2 diffusivity in cedar (6.86×10^{-10} m^2 s^{-1}), with tracheid-wood
392 anatomy, was lower than in oak and maple trees (2.22 and 3.63×10^{-9} m^2 s^{-1}), with ring- and diffuse-porous
393 wood anatomy, respectively (Figure 4). To the best of our knowledge, there is only one study in which radial
394 xylem CO_2 diffusivity has been directly measured in fresh wood (Sorz & Hietz 2006). In that study,
395 measurements performed in six species showed that inter-specific differences in diffusivity were largely
396 explained by wood anatomy. Consistent with our results, radial xylem CO_2 diffusivity was lowest in
397 conifers, intermediate in ring-porous species and highest in diffuse-porous species.

398 According to Fick´s law of diffusion, there is a second factor that determines the diffusion of xylem CO_2 to
399 the atmosphere: the [CO_2] gradient along the stem-atmosphere continuum. Xylem [CO_2] is directly related
400 to the respiratory activity of xylem parenchyma and largely determines this gradient, as [CO_2] is 1-2 orders
401 of magnitude greater in the xylem relative to that in the atmosphere (Teskey *et al.* 2008). Measurements
402 performed in ancillary trees showed that xylem [CO_2] in cedar (3.5%) was c. 2.5 and 3.5 times smaller than
403 that in maple and oak trees, respectively (Figure 5). Accordingly, a compilation of xylem [CO_2] data (in the
404 gas phase) reports a lower measurement range in conifers (0.9-8.1 %) relative to angiosperms (3.6-12.1 %)
405 (Table 1 in Teskey *et al.*, 2008). Consistently, a global meta-analysis has shown that parenchyma tissue
406 fraction (integrating ray and axial parenchyma) in xylem is 3.5 times smaller in conifers relative to
407 angiosperms (7.6 and 26.3 %, respectively; Morris *et al.*, 2016), which may determine relatively limited
408 xylem respiration. These two factors together, (1) radial xylem CO_2 diffusivity and (2) diffusive gradients
409 determined by xylem parenchyma fraction and associated respiratory costs, explain inter-specific and

vertical variability in label efflux observed here along the stem and supported our first hypothesis. High diffusivity and high [CO_2] gradients in oak facilitated rapid label loss and vertical reductions in label efflux. Contrastingly, low diffusivity and low [CO_2] gradients in cedar likely retained the label within the xylem, leading to homogeneous label efflux along the stem. More importantly, this study helps to reconcile contrasting observations between conifer and angiosperm species regarding the fate of xylem-transported CO_2. For conifers, large barriers to radial diffusion determined by tracheid wood anatomy (Sorz & Hietz 2006), together with limited stem-atmosphere CO_2 gradients (Teskey *et al.* 2008) ascribed to low maintenance respiration costs of a small fraction of xylem parenchyma (Morris *et al.* 2016), may disconnect CO_2 pools inside and outside the cambium layer (Ubierna *et al.* 2009; Tarvainen *et al.* 2020), thereby decoupling xylem [CO_2] from E_A. On the other hand, high radial diffusivity in species with vessel-wood anatomy (Sorz & Hietz 2006), together with greater xylem respiration and radial [CO_2] gradients (Teskey *et al.* 2008; Morris *et al.* 2016), may to a greater extent link xylem CO_2 pools with E_A in angiosperms.

Assimilation of xylem-transported CO_2

To avoid equivocal detection of non-assimilated ^{13}C–bicarbonate remaining in xylem sap or living cells after infusion, samples were acid washed prior to isotopic analysis (Teskey *et al.* 2017). Tissue ^{13}C enrichment is therefore a consequence of photosynthetic (Ávila *et al.* 2014; De Roo *et al.* 2020b) or anaplerotic (Hibberd & Quick 2002; Hilman *et al.* 2019) C fixation. To evaluate inter-specific and spatial variability in tissue enrichment, the slope of the relationship between label infused and $\delta^{13}C_{\text{vs baseline}}$ was compared (Figure 6). A large gradient in infused label was achieved for oak, likely explaining why significant relationships were only found for this species. Tissue enrichment was highest in bark tissues of the stem denoting (1) progressive depletion of the label reaching distal organs and hence greater enrichment in organs located closer to the labelling point (Ford *et al.* 2007; McGuire *et al.* 2009; Bloemen *et al.* 2013b), and (2) greater photosynthetic and anaplerotic potential for C assimilation in bark relative to xylem tissues, as previously observed in different species (McGuire *et al.* 2009; Bloemen *et al.* 2013a b) likely due to higher chlorophyll content in tissues located outside the cambium layer (Teskey *et al.* 2008; Ávila *et al.*

2014). It is worth noting, however, that in oak canopy shoots where the bark is thin and more permeable to light transmission, the relationship between label infused and enrichment did not differ between bark and xylem tissues. For maple trees, label assimilation was not detectable, likely as a consequence of limited solution uptake, and hence low potential for label assimilation in relation to its limits of detection. For cedar trees, significant tissue enrichment was detected in some cases, but it was unrelated to solution uptake suggesting heterogeneous potential for CO_2 recycling among different trees and even at the organ and tissue level.

Upscaling sample enrichment to the whole tree level (Figure 7) yielded estimates for label assimilation efficiency of 8.7, 0.1 and 20.6 % for cedar, maple and oak, respectively. These percentages, however, might be slightly higher, as label assimilation below 21 ppm throughout different biomass C pools remained undetectable and hence was not taken into account. Substantial solution uptake in cedar and oak trees facilitated estimation of CO_2 recycling efficiency for comparison, with percentages falling within the range of reported values for *P. deltoides* trees (from 5.6 to 17.4%; Bloemen *et al.*, 2013a) and *P. occidentalis* branches (35%; McGuire *et al.*, 2009). For a comparable amount of label infused into cedar and oak trees, total ^{13}C assimilation was on average 2-3 fold smaller in cedar. This comparison refutes our second hypothesis: CO_2 recycling efficiency was not related to low radial xylem CO_2 diffusivity, which could have potentially increased CO_2 availability to fuel woody tissue photosynthesis. As mentioned above, less xylem parenchyma and associated respiratory costs in cedar stems likely counterbalanced lower radial xylem CO_2 diffusivity, hereby limiting CO_2 build-up within the stem. Nevertheless, availability of endogenous CO_2 (relatively high in comparison to atmospheric [CO_2]) might not be the most limiting factor for woody tissue photosynthesis, and additional factors such as bark permeability to light transmission (Cernusak & Cheesman 2015) and chlorophyll content in stem tissues (Ávila *et al.* 2014) might play a more important role in CO_2 recycling efficiency. For both cedar and oak trees, most of the assimilated label was found in bark and xylem tissues of the stem. The large fraction found in stem bark can be attributed to its high photosynthetic activity and consequent tissue enrichment, while the large fraction in stem xylem is related

to its high proportion of biomass. Remarkably, and regardless of inter-specific and spatial variability in enrichment throughout organs and tissues, its mere occurrence in 3-4 m tall trees confirms the ability of both cedar and oak to recycle root-respired CO_2, as firstly observed in *P. deltoides* (Bloemen *et al.* 2013a). The contribution of recycling photosynthesis in woody tissues to overall tree C assimilation might be small under well-water conditions (< 6%; Ford *et al.*, 2007; McGuire *et al.*, 2009; Bloemen *et al.*, 2013b). Nevertheless, its relative unresponsiveness to drought-stress when leaf C assimilation is limited (Cernusak & Marshall 2000; De Roo *et al.* 2020b), make it a reliable and immediate C source to maintain NSC pools at the branch level (De Roo *et al.* 2020a) and xylem hydraulic functionality (Schmitz, Egerton, Lovelock & Ball 2012; De Baerdemaeker, Salomón, De Roo & Steppe 2017), thereby acquiring an increasingly important role under changing and drier climates.

Gaining perspective at the whole tree level

Most of the labelled C infused into cedar trees remained undetected (56 %, Figure 8), so it did not efflux to the atmosphere from the stem nor it was significantly assimilated throughout the plant. Low radial xylem CO_2 diffusivity and diffusive force led to limited label efflux from the stem (35 % of the total C infused), therefore facilitating label transport upwards to the canopy. As no substantial evidence of label reaching foliar tissues was found, a large fraction of the label might have been lost along intermediate positions; i.e., woody organs within the canopy. It is also possible that part of the label was assimilated along the proximal end of branches (location not sampled), or remained in the xylem and other parts of the plant as bicarbonate. We suggest that tree branching architecture may play a role in the emission of xylem-transported CO_2 at the whole tree level. According to Fick´s law of diffusion, the third and last factor determining diffusion fluxes is the length of the diffusive pathway. When xylem-transported CO_2 moves from the stem into the branch, the reduction in sapwood thickness of the conducting organ leads to a parallel reduction in the radial diffusive pathway, which may cause a large release of xylem-transported CO_2 along the stem-branch transition. Supporting this hypothesis, more and thinner branches were counted in cedar (48 ± 3 branches $tree^{-1}$ and 8.4 ± 0.3 mm, respectively; Figure S2) relative to oak trees, with less and thicker branches (23 ±

2 branches tree^{-1} and 10.8 ± 0.6 mm). Profuse branching in cedar trees may partly explain the large fraction of undetected label, likely emitted to the atmosphere along the stem-branch transition and downstream. On the other hand, high diffusivity and diffusive force in maple and oak trees led to relatively larger label efflux from the stem (97 and 61 % in maple and oak, respectively), values consistent with a previous study in which 83-94% of the $^{13}CO_2$ infused at the stem base of 7-year-old *P. deltoides* trees was not assimilated throughout above-ground organs and was assumed to be lost via CO_2 diffusion to the atmosphere (Bloemen, McGuire, Aubrey, Teskey & Steppe 2013a). In maple and oak trees, most label efflux occurred in the lower half of the stem, as we could expect from a progressive label depletion along the stem vertical profile. High label efflux through the stem limited label transport towards the canopy, as denoted by the comparatively small fraction of undetected label.

To conclude, three insights can be gained from this study: (1) radial xylem CO_2 diffusivity and xylem [CO_2] were lower in cedar relative to maple and oak trees, suggesting disconnected CO_2 pools inside and outside the cambium in conifer relative to angiosperm species, (2) label assimilation in 3-4 m tall trees suggests recycling of root-respired CO_2 throughout organs and tissues in cedar and oak, which could play a crucial role under drier climates, and (3) tree branching architecture may affect spatial patterns in the efflux of xylem-transported CO_2 at the whole tree level.

Acknowledgements

We thank Philip Deman and Geert Favyts for their inestimable help to prepare and maintain the experimental setup. We also thank Katja Van Nieuland for her work on the isotopic analyses and Nancy Pausenberger for isotopic sample preparation. This project received funding from the FWO and the European Union's Horizon 2020 research and innovation programme under the Marie Skłodowska-Curie grant agreement no 665501 granted to R.L.S, as well as from the Special Research Fund (BOF) of Ghent University for Postdoctoral Fellowships. Additionally, funding was provided by the Research Foundation Flanders (FWO) under Research Programme G.0941.15N granted to K.S. and supporting the research of L.D.R.

Conflict of Interest

We declare no conflict of interests in relation to this work.

References

Aubrey D.P. & Teskey R.O. (2009) Root-derived CO_2 efflux via xylem stream rivals soil CO_2 efflux. *New Phytologist* **184**, 35–40.

Ávila E., Herrera A. & Tezara W. (2014) Contribution of stem CO_2 fixation to whole-plant carbon balance in nonsucculent species. *Photosynthetica* **52**, 3–15.

De Baerdemaeker N.J.F., Arachchige K.N.R., Zinkernagel J., Van den Bulcke J., Van Acker J., Schenk H.J. & Steppe K. (2019) The stability enigma of hydraulic vulnerability curves: addressing the link between hydraulic conductivity and drought-induced embolism. *Tree Physiology* **39**, 1646–1664.

De Baerdemaeker N.J.F., Salomón R.L., De Roo L. & Steppe K. (2017) Sugars from woody tissue photosynthesis reduce xylem vulnerability to cavitation. *New Phytologist* **216**, 720–727.

Bloemen J., Bauweraerts I., De Vos F., Vanhove C., Vandenberghe S., Boeckx P. & Steppe K. (2015) Fate of xylem-transported ^{11}C- and ^{13}C-labeled CO_2 in leaves of poplar. *Physiologia Plantarum* **153**, 555–564.

Bloemen J., McGuire M.A., Aubrey D.P., Teskey R.O. & Steppe K. (2013a) Transport of root-respired CO_2 via the transpiration stream affects aboveground carbon assimilation and CO2 efflux in trees. *New Phytologist* **197**, 555–565.

Bloemen J., McGuire M.A., Aubrey D.P., Teskey R.O. & Steppe K. (2013b) Assimilation of xylem-transported CO_2 is dependent on transpiration rate but is small relative to atmospheric fixation. *Journal of Experimental Botany* **64**, 2129–38.

Bloemen J., Teskey R.O., McGuire M.A., Aubrey D.P. & Steppe K. (2016) Root xylem CO_2 flux: an important but unaccounted-for component of root respiration. *Trees* **30**, 343–352.

Cernusak L.A. & Cheesman A.W. (2015) The benefits of recycling: How photosynthetic bark can increase drought tolerance. *New Phytologist* **208**, 995–997.

534 Cernusak L.A. & Marshall J.D. (2000) Photosynthetic refixation in branches of Western White Pine.
535 *Functional Ecology* **14**, 300–311.

536 Dickinson D., Bodé S. & Boeckx P. (2017) Measuring ^{13}C-enriched CO_2 in air with a cavity ring-down
537 spectroscopy gas analyser: Evaluation and calibration. *Rapid Communications in Mass Spectrometry*
538 **31**, 1892–1902.

539 Fan H., McGuire M.A. & Teskey R.O. (2017) Effects of stem size on stem respiration and its flux
540 components in yellow-poplar (*Liriodendron tulipifera* L.) trees. *Tree Physiology* **37**, 1536–1545.

541 Ford C.R., Wurzburger N., Hendrick R.L. & Teskey R.O. (2007) Soil DIC uptake and fixation in *Pinus*
542 *taeda* seedlings and its C contribution to plant tissues and ectomycorrhizal fungi. *Tree physiology* **27**,
543 375–383.

544 Hibberd J.M. & Quick W.P. (2002) Characteristics of C4 photosynthesis in stems and petioles of C3
545 flowering plants. *Nature* **415**, 451–454.

546 Hilman B., Muhr J., Trumbore S.E., Kunert N., Carbone M.S., Yuval P., … Angert A. (2019) Comparison
547 of CO_2 and O_2 fluxes demonstrate retention of respired CO_2 in tree stems from a range of tree species.
548 *Biogeosciences* **16**, 177–191.

549 Hölttä T. & Kolari P. (2009) Interpretation of stem CO_2 efflux measurements. *Tree Physiology* **29**, 1447–
550 1456.

551 Hubeau M., Thorpe M.R., Mincke J., Bloemen J., Bauweraerts I., Minchin P.E.H., … Steppe K. (2019)
552 High-resolution in vivo imaging of xylem-transported CO_2 in leaves based on real-time 11C-tracing.
553 *Frontiers in Forests and Global Change* **2**, 1–12.

554 Huntingford C., Atkin O.K., Martinez de la Torre A., Mercado L.M., Heskel M.A., Harper A.B., … Malhi
555 Y. (2017) Implications of improved representations of plant respiration in a changing climate. *Nature*
556 *Communications* **8**, 1602.

557 Klein T., Zeppel M.J.B., Anderegg W.R.L., Bloemen J., De Kauwe M.G., Hudson P., … Nardini A. (2018)

Xylem embolism refilling and resilience against drought-induced mortality in woody plants: processes and trade-offs. *Ecological Research*.

Long S. & Hällgren J. (1993) Measurement of CO_2 assimilation by plants in the field and the laboratory. In *Photosynthesis and Production in a Changing Environment: A Field and Laboratory Manual*. (eds D.O. Hall, J.M.O. Scurlock, H.R. Bolhàr-Nordenkampf, R.C. Leegood & S.P. Long), pp. 129–167. Springer, Dordrecht, Netherlands.

Maier C.A. & Clinton B.D. (2006) Relationship between stem CO_2 efflux, stem sap velocity and xylem CO_2 concentration in young loblolly pine trees. *Plant, Cell & Environment* **29**, 1471–1483.

McGuire M.A., Marshall J.D. & Teskey R.O. (2009) Assimilation of xylem-transported ^{13}C-labelled CO_2 in leaves and branches of sycamore (*Platanus occidentalis* L.). *Journal of Experimental Botany* **60**, 3809–3817.

McGuire M.A. & Teskey R.O. (2002) Microelectrode technique for in situ measurement of carbon dioxide concentrations in xylem sap of trees. *Tree Physiology* **22**, 807–811.

Mincke J., Courtyn J., Vanhove C., Vandenberghe S. & Steppe K. (2020) Studying in vivo dynamics of xylem-transported 11CO2 using positron emission tomography. *Tree Physiology* **40**, 1058–1070.

Morris H., Plavcová L., Cvecko P., Fichtler E., Gillingham M.A.F., Martínez-Cabrera H.I., … Jansen S. (2016) A global analysis of parenchyma tissue fractions in secondary xylem of seed plants. *New Phytologist* **209**, 1553–1565.

Ogasa M., Miki N.H., Murakami Y. & Yoshikawa K. (2013) Recovery performance in xylem hydraulic conductivity is correlated with cavitation resistance for temperate deciduous tree species. *Tree Physiology* **33**, 335–344.

Powers E.M. & Marshall J.D. (2011) Pulse labeling of dissolved ^{13}C-carbonate into tree xylem: Developing a new method to determine the fate of recently fixed photosynthate. *Rapid Communications in Mass Spectrometry* **25**, 33–40.

582 R Core Team (2019) R: A language and environment for statistical computing. R Foundation for Statistical
583 Computing.

584 De Roo L., Bloemen J., Dupon Y., Salomón R.L. & Steppe K. (2019) Axial diffusion of respired CO_2
585 confounds stem respiration estimates during the dormant season. *Annals of Forest Science* **76**, 52.

586 De Roo L., Salomón R.L., Oleksyn J. & Steppe K. (2020a) Woody tissue photosynthesis delays drought
587 stress in *Populus tremula* trees and maintains starch reserves in branch xylem tissues. *New Phytologist*
588 **228**, 70–81.

589 De Roo L., Salomón R.L. & Steppe K. (2020b) Woody tissue photosynthesis reduces stem CO_2 efflux by
590 half and remains unaffected by drought stress in young *Populus tremula* trees. *Plant, Cell &*
591 *Environment* **43**, 981–991.

592 Salomón R.L., De Roo L., Bodé S., Boeckx P. & Steppe K. (2019) Isotope ratio laser spectroscopy to
593 disentangle xylem-transported from locally respired CO_2 in stem CO_2 efflux. *Tree Physiology* **39**, 819–
594 830.

595 Salomón R.L., De Roo L., Oleksyn J., De Pauw D.J.W. & Steppe K. (2020) TReSpire – a biophysical TRee
596 Stem respiration model. *New Phytologist* **225**, 2214–2230.

597 Salomón R.L., De Schepper V., Valbuena-Carabaña M., Gil L. & Steppe K. (2018) Daytime depression in
598 temperature-normalised stem CO_2 efflux in young poplar trees is dominated by low turgor pressure
599 rather than by internal transport of respired CO_2. *New Phytologist* **217**, 586–598.

600 Salomón R.L., Valbuena-Carabaña M., Gil L., McGuire M.A., Teskey R.O., Aubrey D.P., … Rodríguez-
601 Calcerrada J. (2016) Temporal and spatial patterns of internal and external stem CO_2 fluxes in a sub-
602 Mediterranean oak. *Tree Physiology* **36**, 1409–1421.

603 Schmitz N., Egerton J.J.G., Lovelock C.E. & Ball M.C. (2012) Light-dependent maintenance of hydraulic
604 function in mangrove branches: Do xylary chloroplasts play a role in embolism repair? *New*
605 *Phytologist* **195**, 40–46.

606 Sorz J. & Hietz P. (2006) Gas diffusion through wood: Implications for oxygen supply. *Trees - Structure*
607 *and Function* **20**, 34–41.

608 Steppe K., Saveyn A., McGuire M.A., Lemeur R. & Teskey R.O. (2007) Resistance to radial CO_2 diffusion
609 contributes to between-tree variation in CO_2 efflux of *Populus deltoides* stems. *Functional Plant*
610 *Biology* **34**, 785–792.

611 Steppe K., Sterck F. & Deslauriers A. (2015) Diel growth dynamics in tree stems: linking anatomy and
612 ecophysiology. *Trends in Plant Science* **20**, 335–343.

613 Stringer J.W. & Kimmerer T.W. (1993) Refixation of xylem sap CO_2 in Populus deltoides. *Physiologia*
614 *Plantarum* **89**, 243–251.

615 Stutz S.S., Anderson J., Zulick R. & Hanson D.T. (2017) Inside out: efflux of carbon dioxide from leaves
616 represents more than leaf metabolism. *Journal of Experimental Botany* **68**, 2849–2857.

617 Stutz S.S. & Hanson D.T. (2019) Contribution and consequences of xylem-transported CO_2 assimilation for
618 C_3 plants. *New Phytologist* **223**, 1230–1240.

619 Tarvainen L., Wallin G., Linder S., Näsholm T., Oren R., Löfvenius M.O., … Marshall J.D. (2020) Limited
620 vertical CO_2 transport in stems of mature boreal Pinus sylvestris trees. *Tree Physiology*.

621 Teskey R.O., McGuire M.A., Bloemen J., Aubrey D.P. & Steppe K. (2017) Respiration and CO_2 fluxes in
622 trees. In *Plant Respiration: Metabolic Fluxes and Carbon Balance*. (eds G. Tcherkez & J.
623 Ghashghaie), pp. 181–207. Springer International Publishing, Cham.

624 Teskey R.O., Saveyn A., Steppe K. & McGuire M.A. (2008) Origin, fate and significance of CO_2 in tree
625 stems. *New Phytologist* **177**, 17–32.

626 Trumbore S.E., Angert A., Kunert N., Muhr J. & Chambers J.Q. (2013) What's the flux? Unraveling how
627 CO_2 fluxes from trees reflect underlying physiological processes. *New Phytologist* **197**, 353–355.

628 Ubierna N., Kumar A.S., Cernusak L.A., Pangle R.E., Gag P.J. & Marshall J.D. (2009) Storage and

transpiration have negligible effects on $\delta^{13}C$ of stem CO_2 efflux in large conifer trees. *Tree Physiology* **29**, 1563–1574.

Valentini R., Matteucci G., Dolman a J., Schulze E.D., Rebmann C., Moors E.J., … Clement R. (2000) Respiration as the main determinant of carbon balance in European forests. *Nature* **404**, 861–865.

Vandegehuchte M.W., Bloemen J., Vergeynst L.L. & Steppe K. (2015) Woody tissue photosynthesis in trees: salve on the wounds of drought? *New Phytologist* **208**, 998–1002.

Yang J., He Y., Aubrey D.P., Zhuang Q. & Teskey R.O. (2016) Global patterns and predictors of stem CO_2 efflux in forest ecosystems. *Global Change Biology* **22**, 1433–1444.

Table 1. Sets of instrumented trees including species, the days of year (DOYs) and the corresponding season during which measurements were performed.

Set	Species	DOYs	Season
A	*Thuja occidentalis*	145-151	Spring
B	*Acer platanoides*	154-164	Spring
C	*Quercus robur*	166-176	Spring
D	*Acer platanoides*	244-250	Late summer
E	*Quercus robur*	252-262	Late summer
F	*Thuja occidentalis*	264-274	Late summer

Within each set of measurements, a non-labelling period of 3-6 days was followed by a labelling period of 4-5 days. Each set of trees was composed by three labelled trees and one non-labelled tree used for ancillary measurements and for isotopic baseline sampling.

643 **Figure 1** Photograph of the setup to infuse tree stems with an aqueous ^{13}C-enriched solution and
644 subsequently track label efflux and assimilation throughout the tree (a). Label solution uptake after 4-5 days
645 of labelling period in cedar, maple and oak trees during spring and late summer (b).

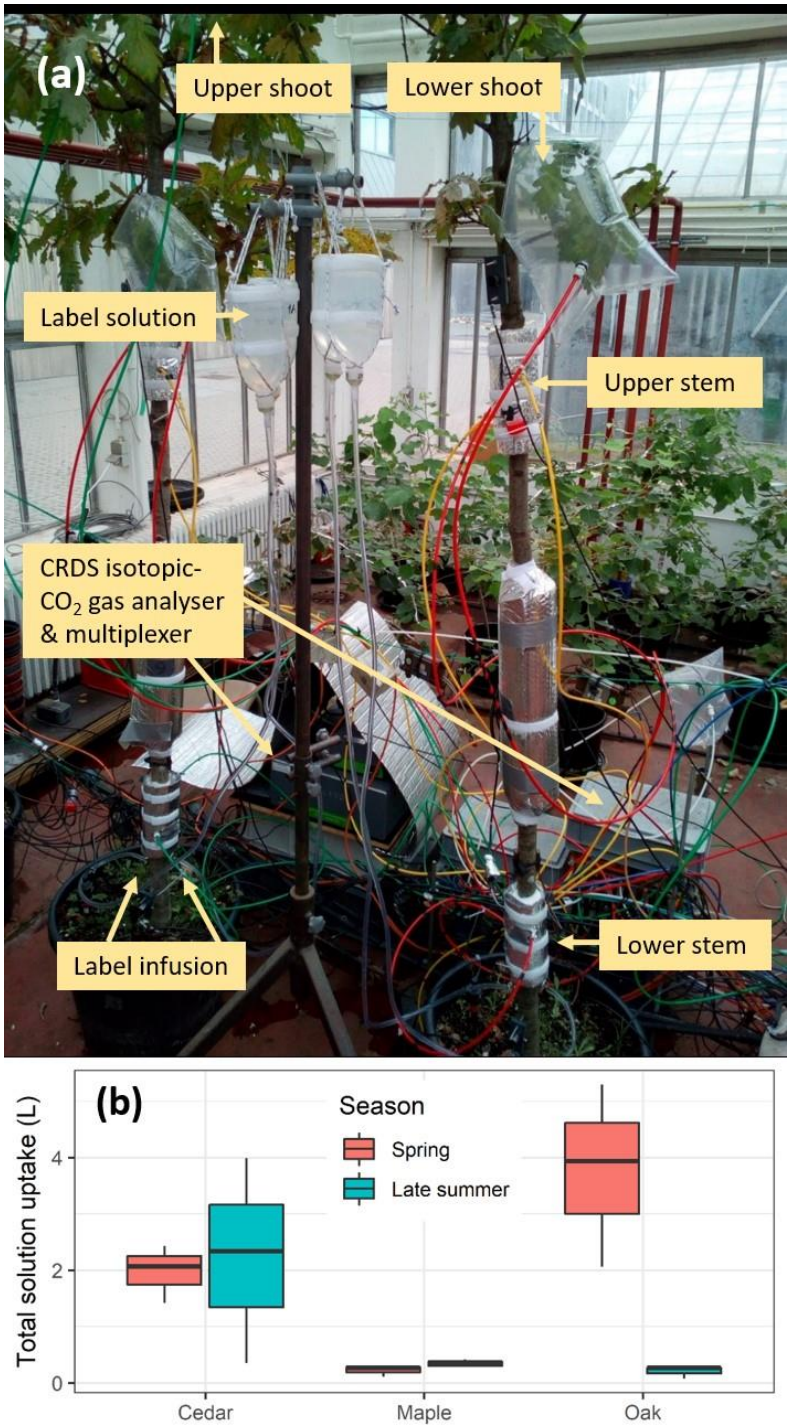

646

Figure 2. Temporal and spatial variability in ^{13}C abundance of air exiting the chambers ($a^{13}C_{CO2,out}$, %) in the lower stem, upper stem and leafy shoots of cedar, maple and oak trees (upper, middle and lower panels, respectively) during spring and late summer (left- and right-hand side panels, respectively).

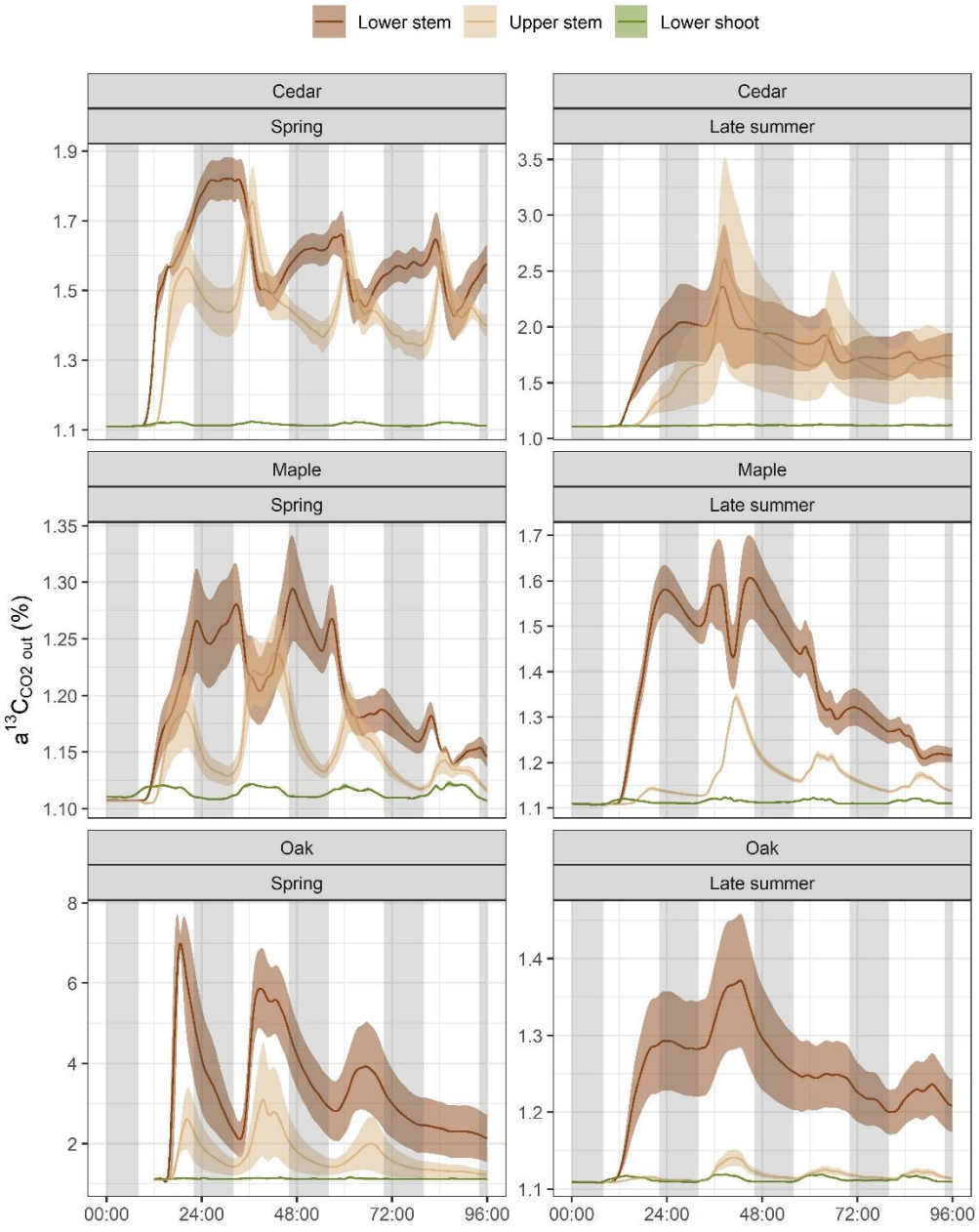

Label infusion started c. at 8:00 h of the 96-h labelling period displayed. Lines and shaded areas represent mean ± SE (n = 3). Grey vertical areas indicate night-time (from 22:00 to 08:00 h).

Figure 3. Relationship between daily label infused and label efflux (on a surface basis) in upper and lower stem sections in cedar, maple and oak trees.

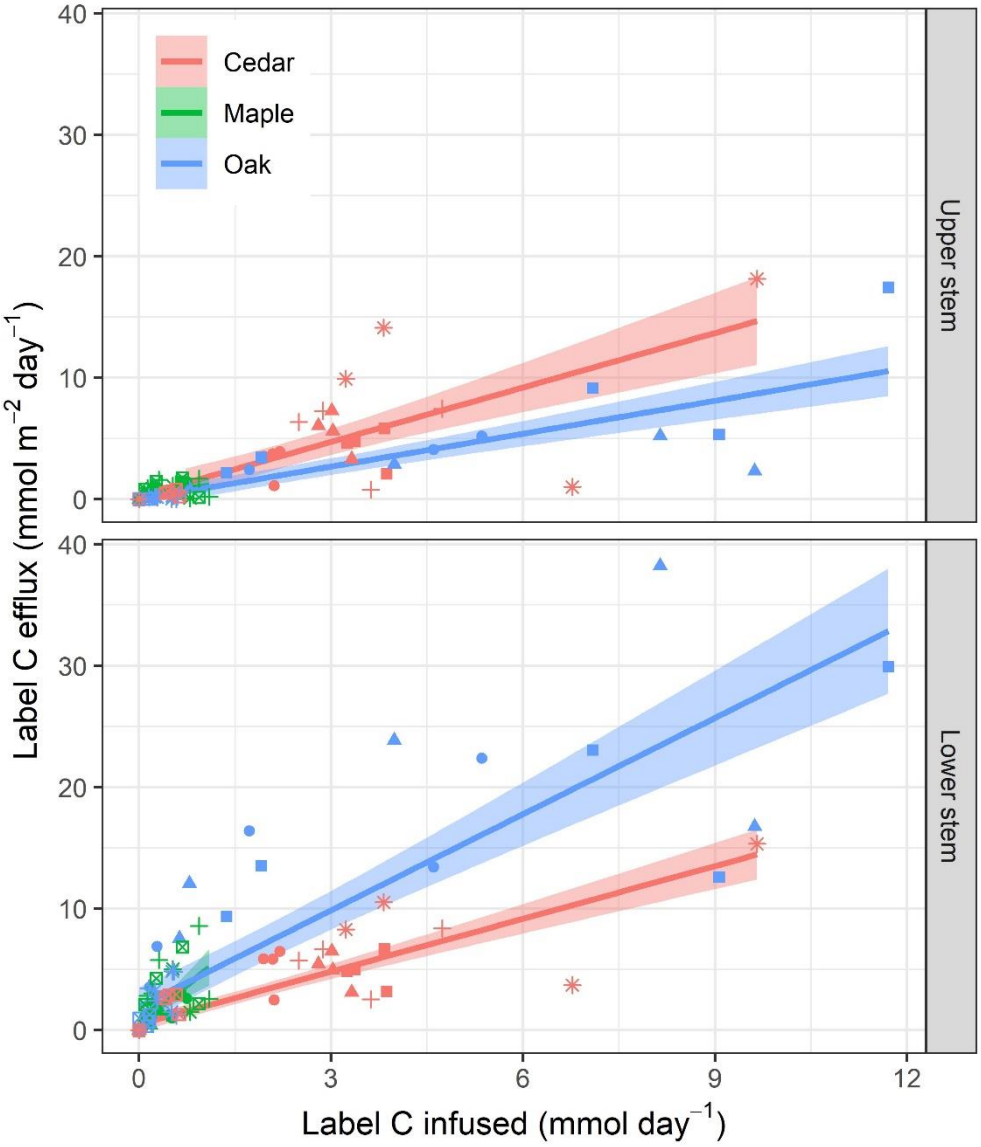

Different trees (n = 6) are displayed with different point symbols.

Figure 4. Radial xylem CO_2 diffusivity in cedar, maple and oak.

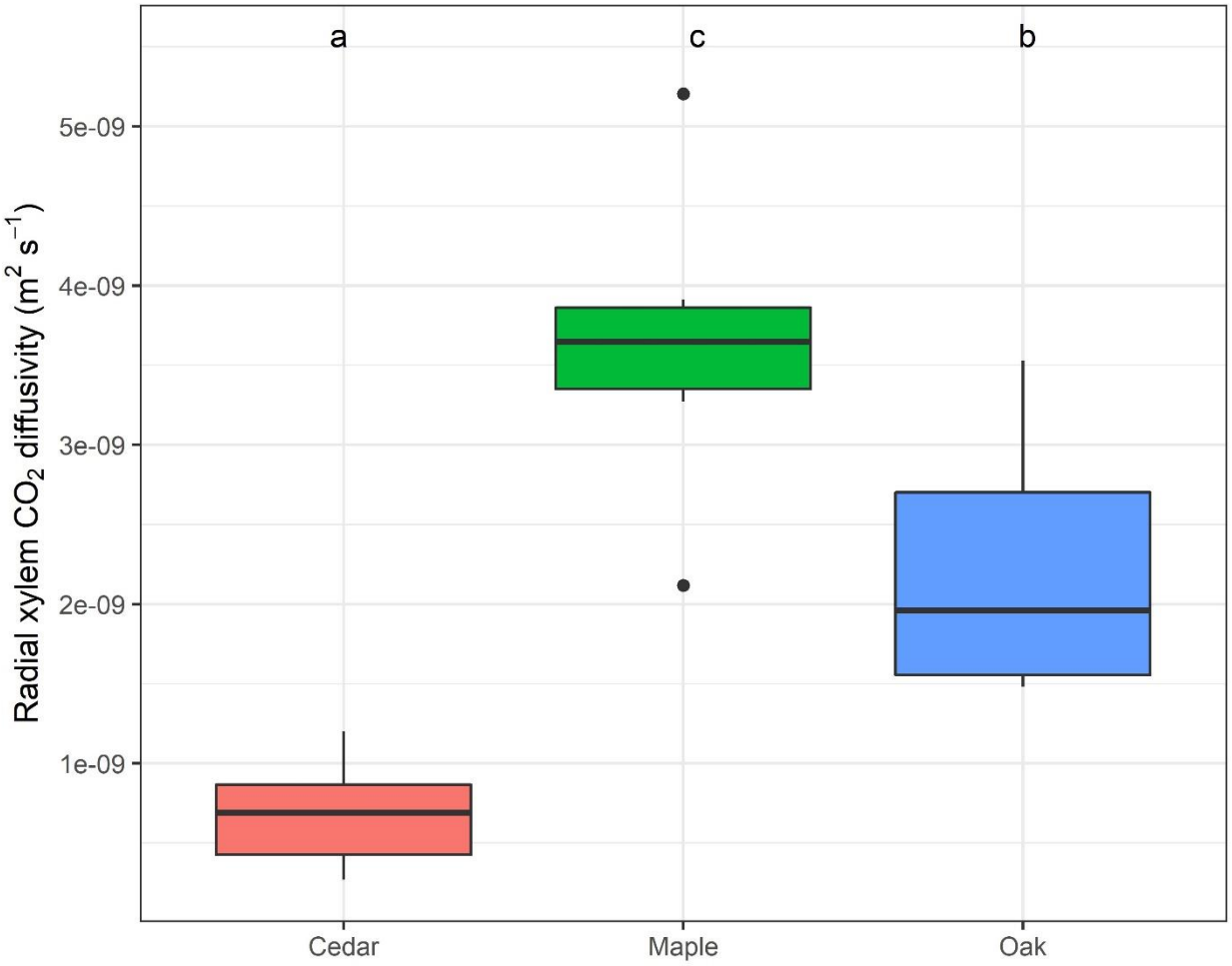

Data from spring and late summer seasons was pooled. Different letters denote significant differences among species (n = 6).

663 **Figure 5.** Concentration of CO_2 measured in the xylem of cedar, maple and oak trees during spring and late

664 summer.

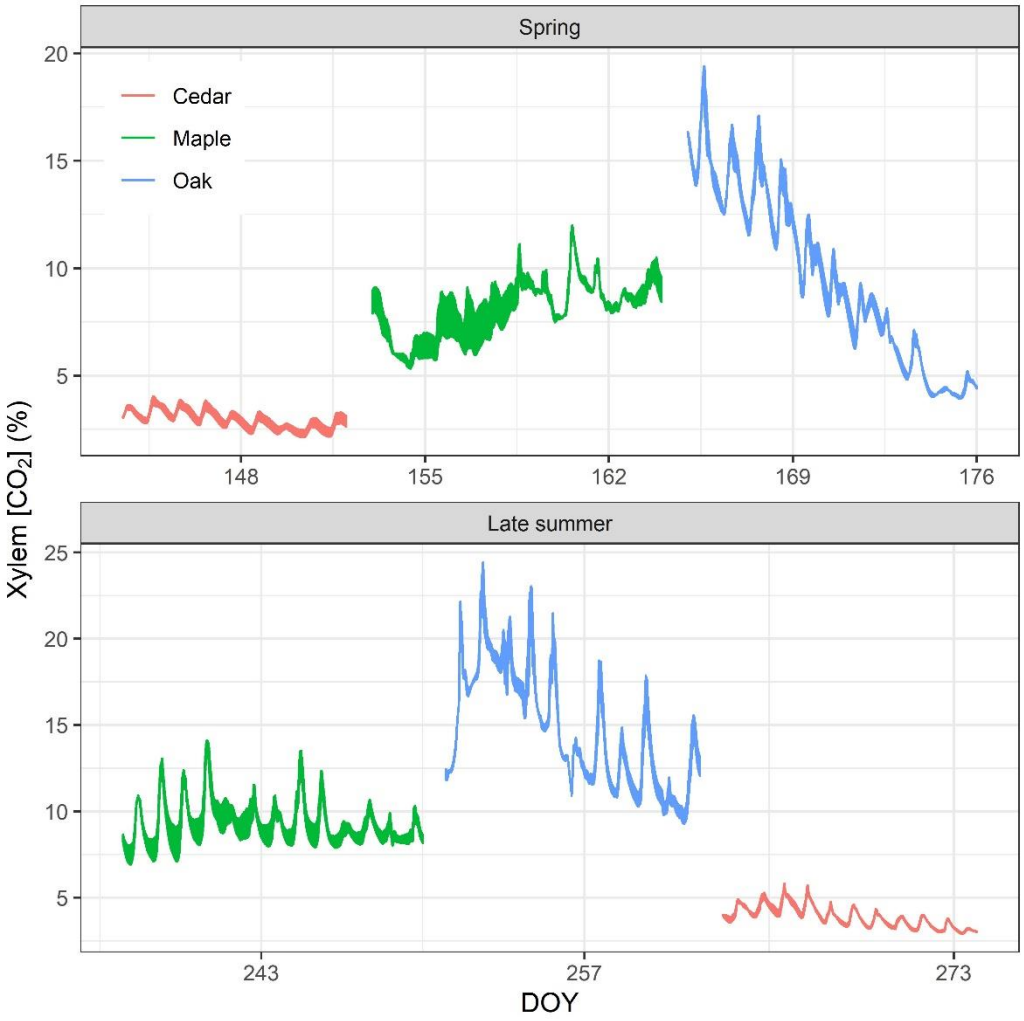

665

666 Bands represent the range of xylem [CO_2] registered along two probes vertically separated by 35-40 cm

667 installed in ancillary (non-labelled) trees used for intrusive measurements.

668

Figure 6. Tissue enrichment ($\delta^{13}C_{vs\ baseline}$) in cedar, maple and oak trees across tree locations (stem, lower shoot and upper shoot) and tissues (xylem, bark and leaves) in relation to total label infused.

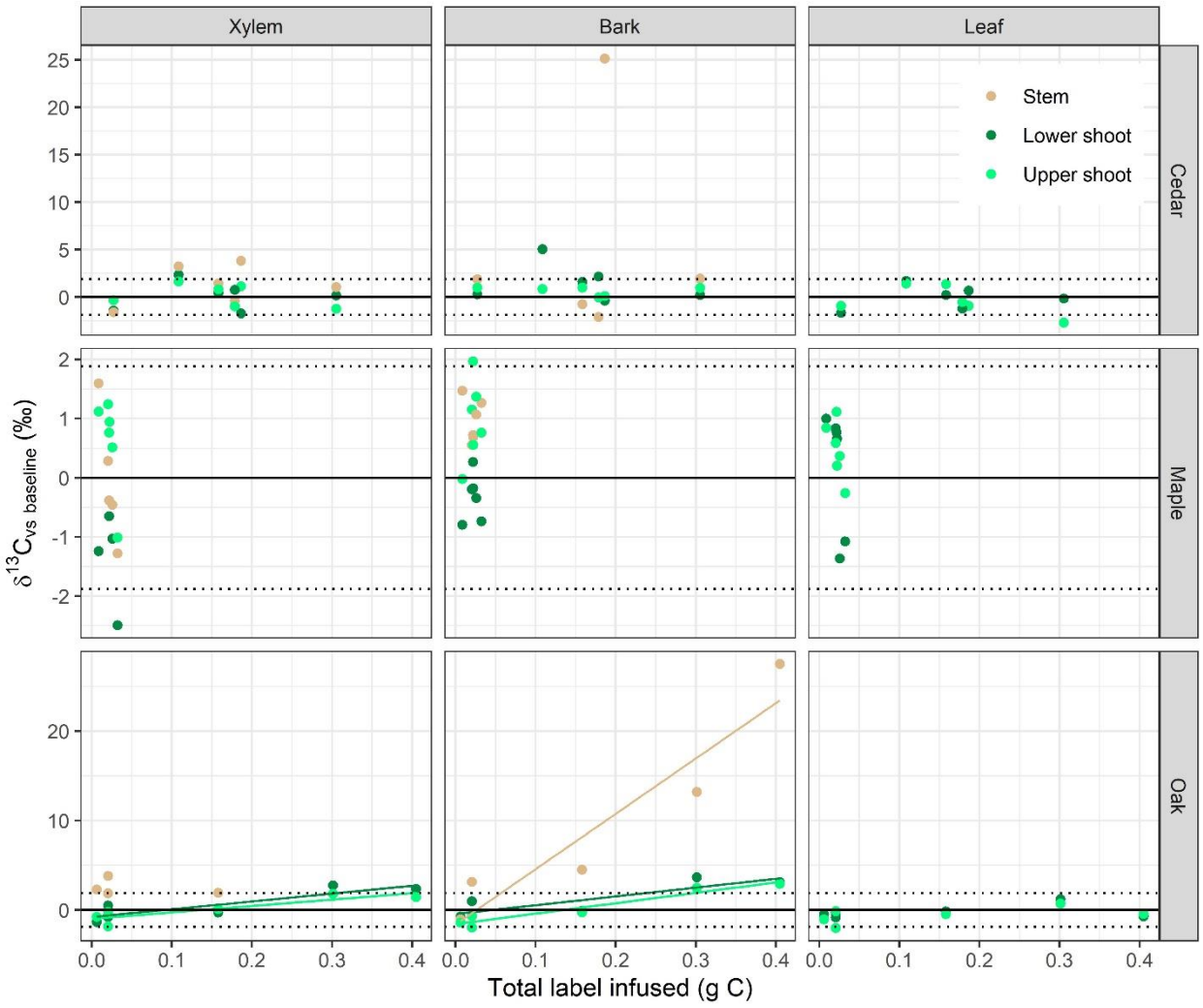

Limits of detection for significant enrichment (1.88 ‰) are shown with dashed lines. In cases of significant relationship between label infused and $\delta^{13}C_{vs\ baseline}$, linear regressions are displayed.

675 **Figure 7.** Biomass partitioning of monitored trees across locations (stem, lower shoots and upper shoots)
676 and tissues (heartwood, xylem sapwood, bark and leaves) (a) and the corresponding mean label assimilation
677 across trees, locations and tissues (b).

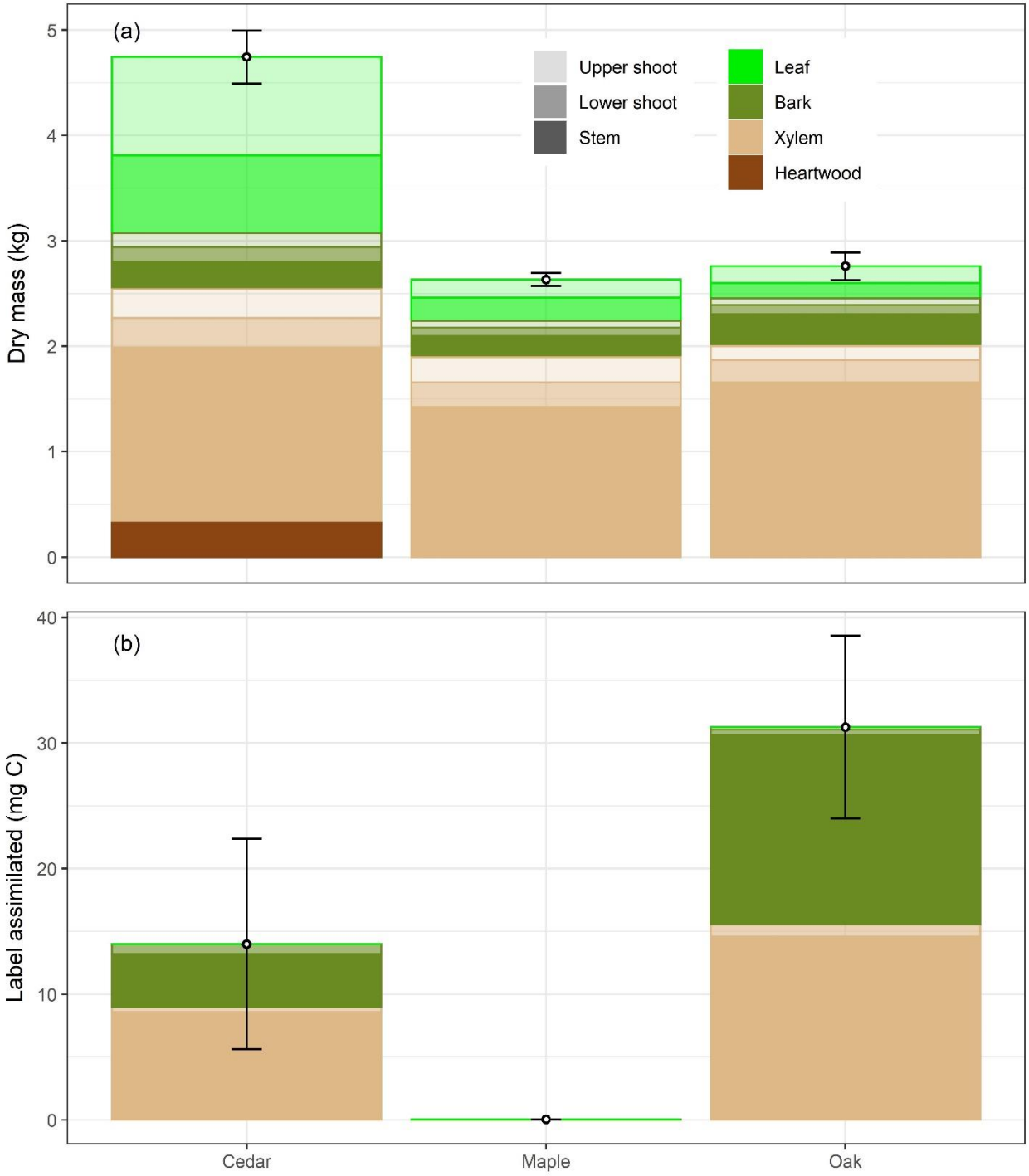

678

Figure 8. Allocation of xylem-transported label into different C sinks in cedar, maple and oak trees.

The amount of label efflux to the atmosphere (E_A; dark and light blue for the lower and upper stem, respectively) and label assimilated (green) is expressed relative to the amount of label infused (%).